Pol. J. Environ. Stud. Vol. XX, No. X (XXXX), 1-14

DOI: *10.15244/pjoes/217443* ONLINE PUBLICATION DATE: 2026-04-16

Original Research

Spatial Distribution and Sources of Heavy Metals in Alluvial Soils of a Typical Area in the Middle Reaches of the Heihe River: A Case Study of Gaotai County, Zhangye City

Yuze Bai[1#°], Yi Liu[1, 2#*], Ning Zhang[1], Jiaxing Sun[1], Miao Liu[1], Kairan Xu[1], Manman Lin[1], Furong Zhai[1]

[1]Environmental Geological Survey Office, Langfang Integrated Natural Resources Survey Center, China Geological Survey, Langfang 065000, China

[2]China University of Geosciences Beijing, Beijing 100000, China

Received: 26 November 2025

Accepted: 27 January 2026

Abstract

The oasis agricultural area in the middle reaches of the Heihe River is a crucial grain production base in Northwest China, and its soil environmental quality is vital for regional ecological security and sustainable agricultural development. This study selected Gaotai County, characterized by a typical "two mountains flanking one river" topography in the middle reaches of the Heihe River, as the research area. Twenty samples were systematically collected from four soil profiles (1 m depth), and the contents of As, Cd, Cr, Cu, Hg, Ni, Pb, and Zn were determined. Comprehensive application of the Potential Ecological Risk Index (RI), chemical weathering indices (CIA, ba), multivariate statistical analysis, and geochemical methods revealed the vertical distribution characteristics, ecological risks, chemical weathering degree, and sources of heavy metals. Results indicated that the soils were overall at a low ecological risk level (RI < 150). However, Cd and Hg were the primary contributors to ecological risk, reaching moderate risk levels at multiple sampling points, thus identified as priority control pollutants. The soils have undergone moderate chemical weathering accompanied by significant potassium metasomatism. Principal Component Analysis (PCA) and correlation analysis indicated spatial heterogeneity in heavy metal sources: profiles P1-P2 were mainly controlled by natural parent material and agricultural sources (Cd), whereas sources for profiles P3-P4 were more complex, primarily a mixture of natural parent material, agricultural sources, and specific industrial/historical sources (Hg). This study elucidates the distribution patterns and sources of heavy metals in alluvial soils under the coupling influence of underlying surface topography and intensive agricultural activities,

# equal contribution

*e-mail: liuyi51861@163.com

°ORCID iD: 0009-0006-9616-9426

providing a scientific basis for the precise prevention, control, and risk management of soil heavy metals in the oasis agricultural areas of the Heihe River Basin.

Keywords: middle Heihe River, alluvial soil, heavy metals, source apportionment, chemical weathering

Introduction

Soil, as a vital component of the environmental ecosystem, directly influences agricultural product safety, ecosystem health, and human well-being [1, 2]. In recent years, with rapid industrialization and intensive agricultural development, soil heavy metal pollution has become a global environmental issue [3, 4]. Due to their toxicity, persistence, bioaccumulation, and non-degradability, heavy metals can accumulate in the human body through the food chain, posing serious threats to the central nervous system, kidney function, and various organs, thereby raising widespread public health concerns [5-7]. Therefore, in-depth research on the spatial distribution, sources, and potential ecological risks of heavy metals in regional soils is crucial for formulating effective soil management policies and ensuring sustainable environmental development.

Numerous studies have been conducted on the distribution, sources, migration, and transformation of heavy metals in soils. Recent research increasingly focuses on the vertical distribution characteristics of heavy metals in soil profiles. These distribution patterns are key to distinguishing natural background levels from anthropogenic inputs [8-10]. Typically, elements controlled by parent material show uniform distribution in the profile, whereas those introduced by human activities often exhibit complex enrichment phenomena, forming intricate vertical distribution sequences [11-13]. At the regional scale, the content and distribution of heavy metals in soils result from the combined effects of natural processes and anthropogenic activities [14-16]. Natural sources primarily include the weathering of parent materials, which determines the geochemical background values of the soil [14, 17, 18]. Anthropogenic sources encompass industrial and mining emissions, agricultural fertilization, wastewater irrigation, traffic emissions, and municipal waste disposal, among others [19-21].

To scientifically assess the degree of pollution, researchers have developed a series of evaluation methods. The geo-accumulation index (I_{geo}), which compares element concentrations to background values while incorporating sedimentological characteristics, effectively quantifies the enrichment effects of anthropogenic activities on the soil environment and has been widely applied in pollution assessments of estuaries, river systems, and agricultural soils [22, 23]. Meanwhile, the Potential Ecological Risk Index (RI), proposed by Håkanson, integrates the toxicity levels of specific heavy metals, their environmental concentrations, and potential ecological synergistic effects [24]. This provides a more comprehensive reflection of the potential biological toxicity impacts of complex multi-heavy metal pollution and has been established as a classical tool internationally for assessing the ecological risks of soils or sediments in regional environments. Globally, numerous studies have successfully utilized the RI to reveal the ecological risk levels and spatial distribution characteristics of heavy metals across different land use types [25, 26]. Precise identification of different sources and quantification of their contribution rates are prerequisites for effectively controlling and remediating soil heavy metal pollution. Accurate source identification is the first step in pollution control. Currently, source apportionment techniques have evolved from qualitative judgment to quantitative calculation. Principal Component Analysis (PCA) and Factor Analysis (FA), which identify groups of elements with common sources through dimensionality reduction, are classical methods for preliminary identification of potential source types [27, 28]. Cluster Analysis (CA) is used to classify samples or elements, identifying areas with similar pollution characteristics. The Positive Matrix Factorization (PMF) model is currently a mainstream tool for source apportionment internationally [29-31]. It can quantitatively calculate the contribution rates and composition profiles of various pollution sources directly using environmental sample data without prior knowledge of source profiles, enabling precise tracing from "source" to "sink". Zhang et al. [32] employed the Potential Ecological Risk Index (RI) and Positive Matrix Factorization (PMF) model to assess the characteristics and sources of heavy metals in riparian soils of an alpine region. Their findings indicated that cadmium (Cd) was primarily influenced by traffic and agricultural activities, while chromium (Cr) and nickel (Ni) were affected by pedogenic parent material weathering and agricultural practices. Lead (Pb) and zinc (Zn) origins were linked to traffic emissions and geological background, and copper (Cu) was predominantly associated with industrial and mineral resource development activities. Previous studies have commonly integrated these multiple analytical methods, systematically revealing the pollution status, ecological risks, and primary sources of soil heavy metals across different global scales, thereby providing critical scientific support for regional environmental management [22, 33, 34].

Oasis agricultural ecosystems in inland river basins, especially in arid and semi-arid regions, are highly sensitive to environmental changes and human disturbances. The Heihe River Basin, a typical inland river basin in arid Northwest China, has its middle reaches serving as an important production base for grain and economic crops in the Hexi Corridor [35, 36]. However, in pursuit of high agricultural yields, the application of chemical fertilizers and pesticides in this region has significantly increased over the past few decades [37, 38]. Concurrently, urbanization and industrialization may have introduced new pollution sources. These activities may lead to the accumulation of heavy metals such as Cd, As, Pb, and Zn in the soil, threatening the sustainability of this fragile oasis ecosystem [37, 39, 40].

Although some studies have focused on the soil environmental quality of the Heihe River Basin, most have either examined the macro-scale of the entire basin or focused on the upper reaches affected by mining and the terminal lake area in the lower reaches [40-42]. Research on heavy metals in the soils of the typical agricultural oasis areas in the middle reaches of the Heihe River, represented by Gaotai County, remains limited. In particular, there is a notable lack of studies that integrate the Potential Ecological Risk Index (RI) with multivariate statistics for the systematic source apportionment of heavy metals throughout soil profiles. The unique “two mountains flanking one river” topographic pattern (Qilian Mountains to the south, Heli Mountains to the north, with the main stream of the Heihe River flowing through) profoundly influences the migration and enrichment of materials: the southern Qilian Mountains provide the main source of soil-forming materials, while the northern mountains form a natural barrier, with human agricultural activities highly concentrated on the alluvial plain between them. The strong coupling of natural and anthropogenic factors makes this area a natural laboratory for studying the “source-sink” relationship of heavy metals. Currently, the spatial distribution patterns and source allocation of heavy metals in the alluvial soils under this specific topography and intense anthropogenic disturbance remain unclear.

This study selected Gaotai County in the middle reaches of the Heihe River as a representative case, targeting the alluvial soils within its distinctive “two mountains flanking a river” topographic unit. For the first time, the vertical distribution and source apportionment of heavy metals in soil profiles across this distinct geomorphic setting were investigated. The contents of key heavy metal elements (Cd, As, Pb, Cu, Zn, Ni, Cr, Hg) in the surface soils of the study area were systematically measured, and their pollution levels as well as potential ecological risks were assessed. Comprehensive application of multivariate statistical analysis and geochemical methods was used to accurately identify the main sources of heavy metals. Finally, combining the “two mountains flanking one river” topographic features and geological background of the study area, the controlling mechanisms of natural processes and human activities on the spatial differentiation of heavy metals were thoroughly discussed. The results of this study are expected to provide a scientific basis for soil environmental protection and the prevention and control of heavy metal pollution in the oasis agricultural areas of the middle Heihe River, while also offering a reference research case and management experience for inland river basins with similar topography and development patterns.

Materials and Methods

Study Area

This study selected Gaotai County, located in the middle reaches of the Heihe River in Northwest China, as the typical study area (Fig. 1). Gaotai County

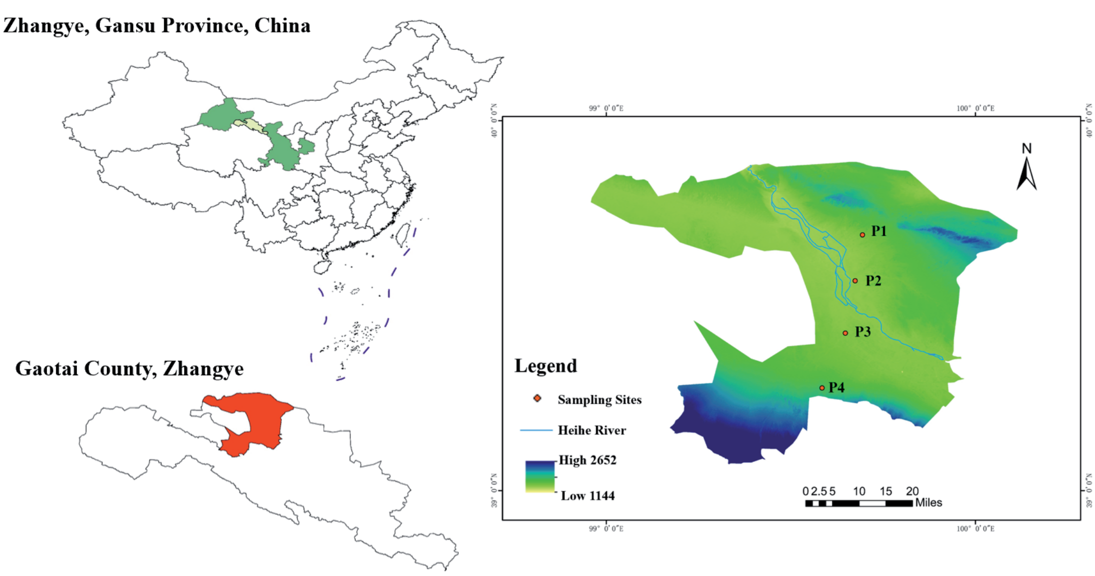

Fig. 1. Distribution of sampling sites.

is situated in Zhangye City, Gansu Province, in the core area of the middle Heihe River (approximately 98°57'-100°06'E, 39°03'-39°59'N). The region experiences a typical temperate continental arid climate, with an average annual sunshine duration of over 3,000 hours, an average annual temperature of 8.1ºC, an average annual rainfall of 112.3 mm, and an average annual evaporation of approximately 1876 mm. The prevailing wind direction is southeast. These climatic conditions result in generally alkaline soils, low organic matter content, and noticeable wind erosion in the study area.

The most prominent topographic feature of the study area is the macro-pattern of "two mountains flanking one river". The north is bounded by the Heli Mountains, part of the Beishan Mountain range, while the south is dominated by the majestic Qilian Mountains. These two major mountain systems form the basic tectonic framework of the region and control the general direction of material migration. The main stream of the Heihe River, originating from the glaciers of the Qilian Mountains, flows from south to north through Gaotai County, forming a vast and fertile alluvial plain within the narrow strip between the mountains. This geomorphological pattern is a key factor controlling the soil parent material sources, geochemical background, and material transport in the study area. Its unique topography and active human activities make it an ideal site for studying the environmental behavior of heavy metals in alluvial soils.

Sample Collection and Analysis

Sample Collection

To thoroughly investigate the vertical distribution characteristics and sources of heavy metals in the alluvial soils of the middle Heihe River, this study adopted a soil profile sampling strategy. Sampling was conducted in August 2025 to minimize direct impacts to topsoil from agricultural activities.

Based on the "two mountains flanking one river" topography of Gaotai County, four representative soil profiles (labeled P1-P4) were systematically established from south to north, with their locations shown in Fig. 1.

P1: Located near the foothills of the Qilian Mountains, within the upper part of the alluvial fan. This site represents a unit dominated by inputs from natural weathering sources and strongly influenced by modern fluvial deposition, serving to reflect the initial geochemical background of the southern source material.

P2: Situated in the central part of the alluvial plain, at a distance from the river channel but within the primary irrigation zone. This site represents a typical core area of intensive agriculture. Profoundly influenced by human agricultural activities, it is a key location for identifying heavy metal inputs from agricultural sources.

P3: Located in the north-central part of the alluvial plain, closer to residential areas and historical farmlands. This site represents a transitional zone subject to the combined influence of agriculture and potential historical pollution. It aims to investigate whether heavy metal sources exhibit more complex mixed characteristics under intense anthropogenic disturbance.

P4: Situated at the marginal zone of the alluvial plain near the front of the Heli Mountains. This represents an area potentially influenced by the topographic terminus and groundwater discharge. This location helps identify whether the enrichment of heavy metals in deeper soils is affected by historical legacy pollution or locally heterogeneous parent materials.

At each selected profile point, a soil profile pit of 1.2 m depth was manually excavated, and a fresh, smooth observation face was prepared. Subsequently, following the soil genetic horizons strictly, samples were collected from each clearly identified layer from top to bottom using a clean stainless steel shovel. Using the equidistant sampling method, samples were collected from five depth intervals: 0-20 cm (surface), 20-40 cm, 40-60 cm, 60-80 cm, and 80-100 cm. Within each depth interval, no less than 500 g of soil were uniformly collected from the profile face to form a composite sample. This aimed to obtain a representative sample for each depth interval while reducing the effects of micro-heterogeneity. Ultimately, 20 soil samples were obtained from 4 profiles with 5 depths each. During sampling, all samples were placed into clean polyethylene zip-lock bags with labels containing the profile number, sampling depth, and date. The sealed sample bags were immediately placed in a portable cooler and transported to the laboratory for subsequent processing.

Sample Preparation and Analysis

Laboratory testing was performed at the Analytical Testing Center of the Langfang Natural Resources Comprehensive Survey Center, China Geological Survey. To determine the total heavy metal content, samples were pre-treated using the four-acid (HNO_3-HF-$HClO_4$-HCl) digestion method [16]. Specifically, 0.2 g of soil sample passed through a 100-mesh sieve were accurately weighed into a polytetrafluoroethylene (PTFE) crucible. The four acids were added sequentially, and the mixture was heated on an electric hotplate following a specific temperature program until the sample was completely dissolved and the solution became clear and transparent. After cooling, the digestate was transferred to a volumetric flask and made up to volume with ultrapure water for measurement.

The concentrations of various heavy metal elements (Cd, As, Pb, Cr, Ni, Cu, Zn, Hg) in the digestate were determined using Inductively Coupled Plasma Mass Spectrometry (ICP-MS, Thermo Scientific iCAP RQ). To ensure the accuracy and precision of the analytical data, each batch (every 20 samples) included procedural blanks, national standard soil reference materials (GSS series), and randomly inserted duplicate samples (duplication rate not less than 10%). The recovery rates for all determined heavy metal elements fell within the range of 90%-110% of the certified values of the national standard reference materials, and the relative standard deviation (RSD) of duplicate samples was less than 5%, indicating reliable and quality-controlled analytical data.

Data Treatment and Processing

Assessment of Potential Ecological Risk Index (RI)

To assess the degree of potential ecological harm caused by heavy metals in the soil, this study employed the Potential Ecological Risk Index (RI) method proposed by Håkanson [24]. This method comprehensively considers the toxicity of individual heavy metals, their concentration levels in the environment, and their potential synergistic effects on the ecosystem. The calculation formula is as follows:

$$RI = \sum_{i=1}^{m} E_r^i = \sum_{i=1}^{m} T_r^i \frac{C^i}{C_n^i} \quad (1)$$

Where, C^i is the measured concentration of heavy metal element *i* in the soil (mg/kg); C_n^i is the reference value for that element. Given the lack of official soil environmental background values for the study area, this study used the average heavy metal content in the surface alluvial soils of the Heihe River Basin as the reference value to better approximate the regional geochemical background. T_r^i is the toxic response factor of the element. This study adopted the standardized toxicity coefficients recommended by Håkanson: Hg = 40, Cd = 30, As = 10, Pb/Cu/Ni = 5, Cr = 2, Zn = 1 [24]. The E_r^i is classified into five categories in accordance with the reference [43]: E_r^i<40 (low risk), 40≤E_r^i<80 (moderate risk), 80≤E_r^i<160 (considerable risk), 160≤E_r^i<320 (high risk), and E_r^i≥320 (very high risk). The RI is divided into the following four categories [43]: *RI*<150 (low risk), 150≤*RI*<300 (moderate risk), 300≤*RI*<600 (considerable risk), and *RI*≥600 (high risk).

Degree of Chemical Weathering and Leaching Coefficient

To investigate the influence of natural weathering processes on the distribution and enrichment of heavy metals in the soil, we calculated the Chemical Index of Alteration (CIA) and the base leaching coefficient (ba).

The Chemical Index of Alteration (CIA) is calculated as follows [44]:

$$CIA = [Al_2O_3/(Al_2O_3 + CaO^* + K_2O + Na_2O)] \times 100 \quad (2)$$

The base leaching coefficient (ba) is calculated as follows [45]:

$$ba = [(CaO^* + K_2O + Na_2O)/Al_2O_3] \times 100 \quad (3)$$

Where, CaO^* represents the CaO content in silicate minerals. The molar content of CaO^* was determined using the method proposed by McLennan (1993) [46].

Principal Component Analysis (PCA)

This study used PCA to identify common factors controlling the sources and distribution of soil heavy metals. The analysis was performed using SPSS 26.0 software. First, the Kaiser-Meyer-Olkin (KMO) test and Bartlett's test of sphericity were conducted on the concentration data of all heavy metals to determine the suitability of the data for PCA. Typically, a KMO value greater than 0.6 and a Bartlett's test p-value less than 0.05 indicate that the data are suitable for factor analysis. PCA extracts several uncorrelated principal components from the original correlated variables through linear transformation; these principal components can explain the maximum variance of the original data. The extracted principal components were subjected to orthogonal rotation using the Varimax method to simplify the factor loading matrix structure, facilitating the interpretation of the potential sources represented by each principal component (e.g., anthropogenic sources, natural parent material sources).

Statistical Analysis

Data statistical analysis was performed using SPSS 18 software. Spearman's correlation coefficient was calculated to determine the associations between soil parameters. The A-CN-K(Al_2O_3-(CaO^*+Na_2O)-K_2O) diagram was plotted using OriginPro 2024 software.

Results and Discussion

Vertical Distribution Characteristics of Heavy Metals in Soil Profiles

The vertical distribution patterns of heavy metals in soil profiles are key indicators for revealing their sources (natural genesis or anthropogenic input) and migration behavior. Through systematic sampling and analysis of four profiles (P1-P4) in Gaotai County, this study revealed the vertical differentiation patterns of As, Cd, Cr, Cu, Hg, Ni, Pb, and Zn in the alluvial soils of the study area, as shown in Fig. 2. The authors found that P1 and P2 shared similar enrichment patterns, while P3 and P4 also showed similarities. In profiles P1 and P2, the concentrations of Cr, Cu, Hg, Ni, Pb, and Zn generally exhibited a pattern of first increasing, then decreasing, and finally stabilizing with soil depth. They tended to stabilize in the deep soil layers

(60-100 cm) and approached the local geochemical background values. In profiles P3 and P4, the concentrations of Cr, Cu, Ni, Pb, and Zn also showed similar overall patterns. This distribution characteristic suggests that these elements might be controlled by the natural parent material, i.e., the geochemical background carried by the alluvial deposits themselves. They primarily reside in the crystal lattices of primary silicate minerals, are relatively stable chemically, and are not easily mobile [47]. Their distribution patterns reflect the good original homogeneity maintained in the profiles after the weathering products from the southern Qilian Mountains source area and the northern Heli Mountain rocks were transported and deposited. The concentrations of As and Cd fluctuated more significantly and without clear patterns, which might reflect the influence of anthropogenic activities. Agricultural sources could be one of the surface input pathways for As, and Cd is a common impurity in phosphate fertilizers [48]. Their enrichment in the soil might be closely related to the long-term intensive agricultural activities in the oasis of the middle Heihe River. Frequent tillage activities continuously mix newly input anthropogenic heavy metals into the plow layer, and the typically alkaline soil conditions make some heavy metal elements prone to form hydroxide or carbonate-bound species and become immobilized [49]. It is noteworthy that the variation patterns of Hg concentration in P3 and P4 were quite different. In P4, the peak Hg concentration occurred at 100 cm depth, while in P3, it occurred at 20 cm depth, showing a certain complexity, possibly influenced by multiple factors simultaneously. Hg might originate from historical atmospheric deposition or pesticide use, or it could be related to the parent material [50].

Pollution Assessment of Heavy Metals in Soil Profiles

To quantitatively assess the comprehensive ecological risk level of heavy metals in the soil profiles, we calculated the Potential Ecological Risk Index (RI) and the contribution rate of each element, with the results shown in Table 1. The comprehensive RI for the four profiles (P1-P4) ranged from 19.96 to 116.90. According to Håkanson's classification standard, all profile RI values were below 150, indicating that the soils in the study area overall were at a "low ecological risk" level. However, the risk degree showed significant spatial heterogeneity both within and between profiles. None of the profiles showed a simple pattern of risk monotonically decreasing with depth. P1 showed an RI peak at 60 cm depth (98.50), the highest RI values for P2 and P3 occurred in the surface layer (0-20 cm), while the highest RI value for P4 occurred at 80 cm depth (110.51). This complex vertical distribution suggests that ecological risk is not solely dominated by surface anthropogenic inputs but may also be significantly influenced by deep processes such as abrupt changes in soil texture, capillary rise due to groundwater fluctuation, historical buried pollution layers, or uneven soil parent material [51]. The average RI values for P3 and P4 were relatively high, with the surface RI value of P3 (116.90) approaching the "moderate risk" threshold (150). This implies that these sites might be subject to stronger anthropogenic disturbance or located in specific geochemical anomaly zones. Considering the regional background, these sites might be closer to residential areas or have historically received wastewater irrigation. Analysis of the contribution rate to RI clearly revealed the relative importance of different heavy metal

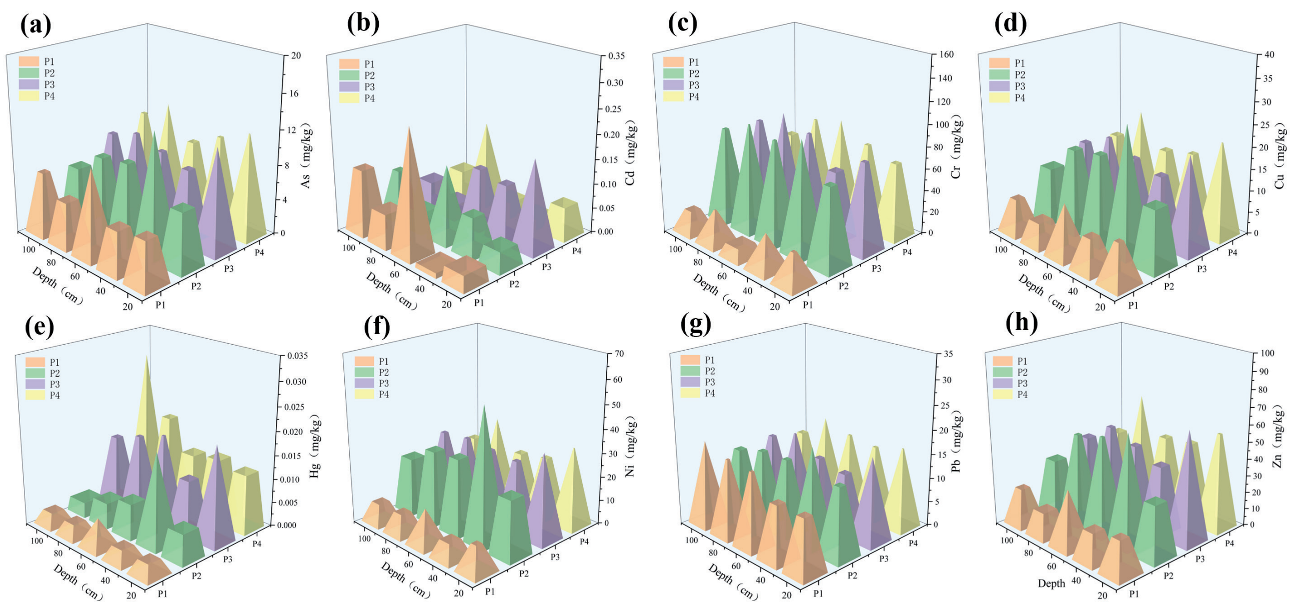

Fig. 2. Vertical distribution of heavy metals in the soil profiles.

elements. In all profiles, Cd and Hg were the two primary ecological risk contributors, together accounting for over 60% to 85% of the RI. The single potential ecological risk factor (E_i) for Cd exceeded 40 in multiple layers, reaching "moderate risk" levels at points such as P1-60 cm (68.18), P2-60 cm (40.91), P3-20 cm (49.09), and P4-80 cm (46.36). Although its absolute concentration might not be high, due to its extremely high toxicity response coefficient (30), Cd became a key ecological risk element in the study area. This corroborates its distribution pattern discussed in previous Section, strongly pointing to agricultural sources, particularly long-term phosphate fertilizer application, as its main input pathway. The ecological risk factor (E_i) for Hg showed characteristics of moderate risk in multiple layers, especially at P2-40 cm (38.00), P3-20 cm (40.00), and P4-100 cm (60.00), reaching "moderate risk" or higher (the value of 60.00 at P4-100 cm is very close to the "considerable risk" threshold of 80). The high value of Hg in the deep layer (P4-100 cm) is an alerting signal, which might reflect the legacy of historical atmospheric deposition, deep leaching of mercury-containing pesticides, or a naturally high background value in the parent material at that point [52]. Its high contribution rate highlights that Hg is a non-negligible potential threat in the oasis environment of the arid region. Compared to Cd and Hg, the ecological risk factors (E_i) for As, Pb, Cu, Ni, Cr, and Zn were generally far below 40, belonging to the "low risk" category. Their combined contribution to RI was typically below 35%. This result confirms that although some elements (As) showed signs of anthropogenic influence in their vertical distribution (previous Section), their input intensity has not yet posed a substantial threat to the overall regional ecological risk. The low-risk status of elements like Cu and Ni further confirms the conclusion that their sources are primarily controlled by natural parent material.

Table 1. Potential ecological risk index (RI) of soil profiles.

Profile	Depth (cm)	E_i								RI
		As	Cd	Cr	Cu	Hg	Ni	Pb	Zn	
P1	20	4.47	8.723	0.82	2.02	6.00	1.66	3.21	0.31	27.21
	40	4.09	2.723	0.94	1.61	6.00	1.11	3.211	0.26	19.96
	60	8.44	68.18	0.33	2.54	12.00	2.19	4.30	0.50	98.50
	80	4.33	18.55	0.87	1.18	6.00	1.31	4.40	0.23	36.85
	100	6.03	35.46	0.59	1.69	6.00	1.25	4.86	0.33	56.20
Contribution to RI (%)		11.46	55.98	1.49	3.79	15.08	3.15	8.37	0.68	100
P2	20	5.59	10.91	2.07	2.91	12.00	3.52	4.02	0.48	41.49
	40	11.62	20.73	2.91	6.09	38.00	8.10	5.50	0.96	93.91
	60	7.77	40.91	2.63	4.25	14.00	4.52	4.27	0.84	79.20
	80	7.35	11.18	2.79	4.02	10.00	4.38	4.19	0.78	44.69
	100	5.40	27.27	2.44	2.67	6.00	3.37	3.74	0.48	51.38
Contribution to RI (%)		12.15	35.73	4.14	6.42	25.75	7.69	7.00	1.14	100
P3	20	9.91	49.09	2.30	4.57	40.00	5.23	4.83	0.96	116.90
	40	6.89	30.00	1.80	3.12	22.00	4.16	3.35	0.58	71.90
	60	7.63	32.73	2.50	3.46	36.00	4.23	3.66	0.67	90.88
	80	8.46	8.45	2.80	4.00	32.00	4.39	4.53	0.75	65.38
	100	7.57	15.00	2.37	3.31	28.00	4.21	3.88	0.58	64.94
Contribution to RI (%)		9.87	32.99	2.87	4.50	38.54	5.42	4.94	0.86	100
P4	20	10.00	17.45	1.93	4.55	24.00	4.77	4.61	0.83	68.15
	40	8.80	5.45	2.15	3.57	26.00	3.60	4.16	0.67	54.42
	60	7.42	8.45	2.55	3.27	24.00	3.33	4.33	0.64	53.99
	80	10.34	46.36	2.34	4.74	36.00	4.94	4.83	0.94	110.51
	100	8.63	14.45	1.71	3.14	60.00	3.21	3.46	0.54	95.14
Contribution to RI (%)		11.82	24.12	2.80	5.04	44.48	5.19	5.60	0.95	100

Chemical Weathering and Leaching of the Soils

The chemical weathering process of soil is a key geochemical process controlling the release, migration, and redistribution of elements from parent rocks, profoundly influencing the background content and environmental behavior of heavy metals in soils. To understand the intensity of pedogenesis and its impact on heavy metal distribution in the study area, we calculated the Chemical Index of Alteration (CIA) and the base leaching coefficient (ba), and plotted the A-CN-K(Al_2O_3-(CaO^*+Na_2O)-K_2O) ternary diagram. The CIA values for the four profiles (P1-P4) are shown in Fig. 3. The CIA values for all samples ranged between 54.4 and 65.4, slightly higher than the Upper Continental Crust (UCC) CIA value of 47.9 [53]. According to the classical classification scheme of [44], this CIA range indicates that the alluvial soils in the middle Heihe River have undergone "moderate" chemical weathering. In terms of vertical distribution (Fig. 3a)), the average CIA value in the surface layer (0-40 cm) of most profiles was slightly lower than that in the deep layers (60-100 cm). This trend might be related to anthropogenic disturbances such as periodic irrigation and fertilization in the surface soil, where the input of fresh, insufficiently weathered fine particles might locally weaken the apparent chemical weathering intensity [54]. In contrast, the deep soil more faithfully records the regional chemical weathering processes that occurred over geological history [54]. The base leaching coefficient (ba) is an effective indicator for measuring the leaching loss degree of base cations (CaO^*, Na_2O, K_2O) relative to the inert component Al_2O_3 [45]. The ba values for all samples in this study were less than 1 (Fig. 3b)), directly confirming the leaching loss of mobile elements like Ca and Na during pedogenesis [45]. This finding seems somewhat contradictory to the arid-semi-arid climatic background of the study area, suggesting that the sediments in this region might have inherited the characteristics of intensely weathered products formed under more humid and hot paleoenvironments in their source area (mainly the southern Qilian Mountains).

The A-CN-K ternary diagram provides intuitive evidence for further understanding weathering trends and pedogenic processes, as shown in Fig. 4. All sample points fall between the granite and shale weathering trend lines and clearly shift towards the A-K edge. This distribution pattern reveals two key processes. First is continuous plagioclase weathering. The evolution of sample points from the parent material area towards the A vertex represents the classic weathering path involving plagioclase (rich in Ca, Na) decomposition and leaching loss, leading to the formation of Al-rich clay minerals [55]. Second is significant potassium metasomatism. The distribution of sample points parallel to the A-K edge is a typical signature of potassium metasomatism [55]. Under arid-semi-arid conditions, due to limited precipitation, the leached K^+ ions are not completely removed from the system but, under suitable conditions, are re-adsorbed by 2:1 type clay minerals in the soil or promote the formation of K-rich minerals like illite, leading to secondary potassium enrichment in the profile. For elements primarily hosted in silicate mineral lattices, intense chemical weathering implies considerable decomposition of these minerals, potentially releasing these elements [17]. However, their relatively uniform distribution in the profile ("Vertical Distribution Characteristics of Heavy Metals in Soil Profiles" Section) suggests that the released elements might be re-immobilized in situ or after short-distance migration, or exist as stable residual phases under arid conditions, with their distribution still mainly controlled by the parent material. Furthermore, intense chemical weathering and widespread clay mineral formation provide important adsorption carriers for heavy metals. The generally alkaline soil in the study area further enhances the adsorption capacity of clay

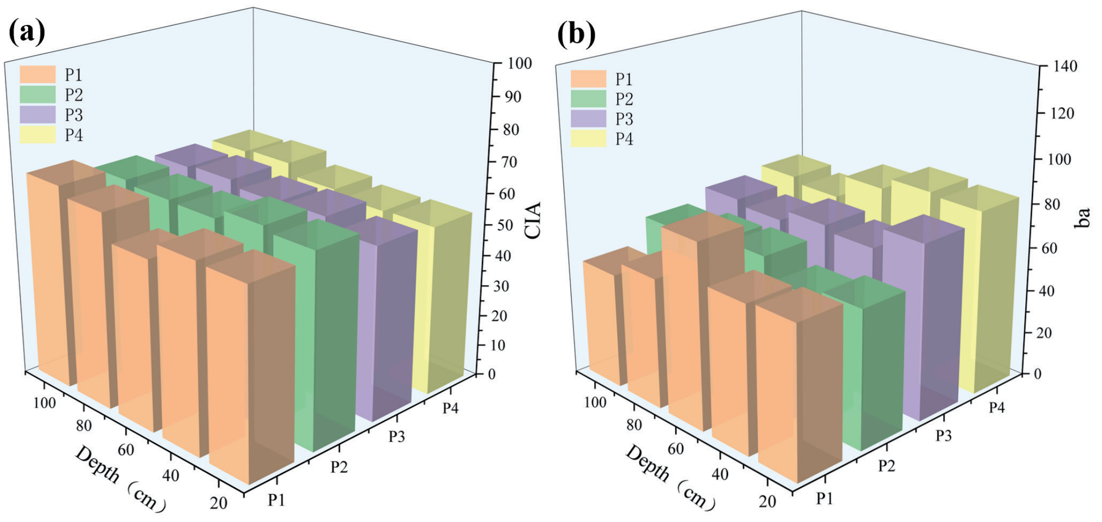

Fig. 3. Variations in different chemical weathering proxies of soil profiles.

minerals and iron-manganese oxides for heavy metal ions like Cd, Pb, and Zn, thereby inhibiting their vertical leaching to some extent and explaining the surface enrichment of some elements [56]. Combining heavy metal data with geochemical indicators like CIA and ba can effectively distinguish anthropogenic inputs from natural weathering contributions. This study observed that the enrichment phenomena of elements like Cd and Hg did not completely align with the overall chemical weathering trend, providing evidence for their anthropogenic sources.

Correlation Analysis and Principal Component Analysis of Heavy Metals in Soil Profiles

To deeply reveal the internal relationships among heavy metal elements in the soil profiles and their potential common sources, we performed Pearson correlation analysis (Fig. 5) and Principal Component Analysis (PCA) (Table 2) for the two profile groups P1-P2 and P3-P4, respectively. The results showed significant differences in the correlation patterns of elements between the different profile groups, further confirming the vertical distribution patterns observed in "Vertical Distribution Characteristics of Heavy Metals in Soil Profiles" Section and revealing more complex source control mechanisms.

In the P1-P2 profile group, correlation analysis (Fig. 5a)) showed significant positive correlations ($p<0.01$) among As, Cr, Cu, Ni, Pb, Zn, Fe_2O_3, and Mn, forming a closely associated element cluster. This finding was strongly supported by the PCA results (Table 2). The first principal component (PC1) explained 72.997% of the total variance and had positive loadings on As (0.340), Cr (0.288), Cu (0.363), Ni (0.361), Pb (0.258), Zn (0.356), Fe_2O_3 (0.352), and Mn (0.331). Fe_2O_3 and Mn are common iron-manganese oxides/hydroxides in soils, which have strong adsorption and co-precipitation effects on heavy metals like Cu, Ni, and Zn. This highly symbiotic relationship indicates that in the P1-P2 profiles, the distribution of these elements is primarily controlled by the weathering products of primary minerals and the geochemical behavior of secondary iron-manganese oxides, reflecting the inherent geochemical background of the Heihe River alluvial deposits. Therefore, the authors attribute PC1 to natural sources. Notably, Cd showed no significant correlation with the aforementioned natural parent material element cluster. In PCA, Cd dominated PC2 (loading 0.721) and PC3 (loading 0.543). This strongly suggests that

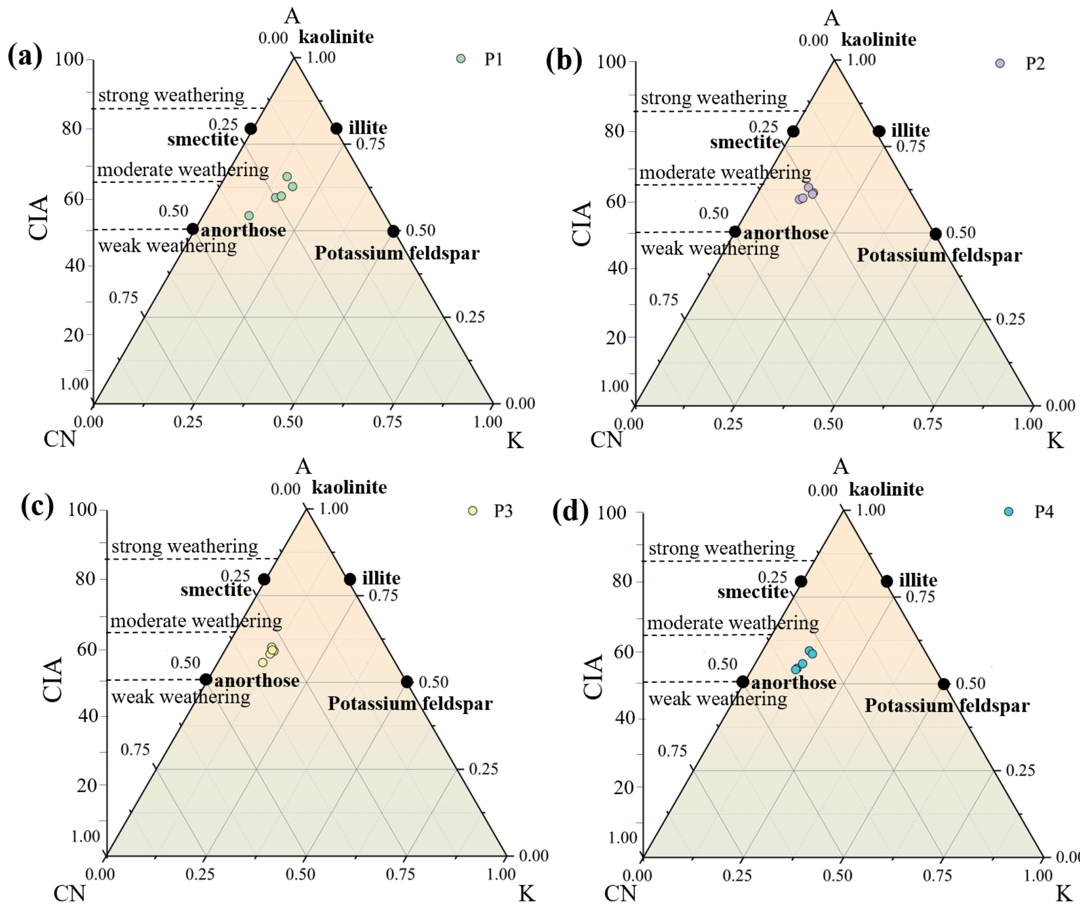

Fig. 4. A-CN-K ternary plot of the soil profile. The axes scales indicate their molar percentages, where A stands for Al_2O_3, CN for $CaO^* + Na_2O$, and K for K_2O.

the input pathways and enrichment mechanisms of Cd are independent of the natural parent material. Phosphate rock used in manufacturing phosphate fertilizers often contains a certain amount of cadmium, and long-term, high-volume application is a key factor leading to Cd accumulation in farmland soils [57]. Additionally, during mineral smelting, Cd, as a volatile impurity, can easily be released into the environment and waste slag. Meanwhile, the authors found that As (0.277) and Pb (0.399) also had positive loadings on PC2, and Zn (0.287) had a positive loading on PC3. Historically, arsenic compounds were widely used as insecticides and herbicides, and their residual effects can persist in soil for a long time [58]. Pb primarily originates from traffic emissions, including the use of leaded gasoline, mechanical wear, etc [58]. Anthropogenic sources of Zn include industrial activities and traffic pollution [58]. Zinc oxide added in tire manufacturing is released into the surrounding soil during wear. Based on previous research findings on heavy metal sources, the authors attribute PC2 to an agricultural-traffic mixed source and PC3 to an agricultural-industrial-traffic mixed source.

The element source patterns in the P3-P4 profile group were more complex. Pearson correlation analysis (Fig. 5b)) showed that Cu, Ni, Pb, Zn, Fe_2O_3, and Mn still exhibited significant positive correlations and jointly dominated PC1 (Table 2), indicating that natural parent material sources remain a fundamental controlling factor in this area. However, the variance contribution rate of PC1 (65.153%) was lower than that

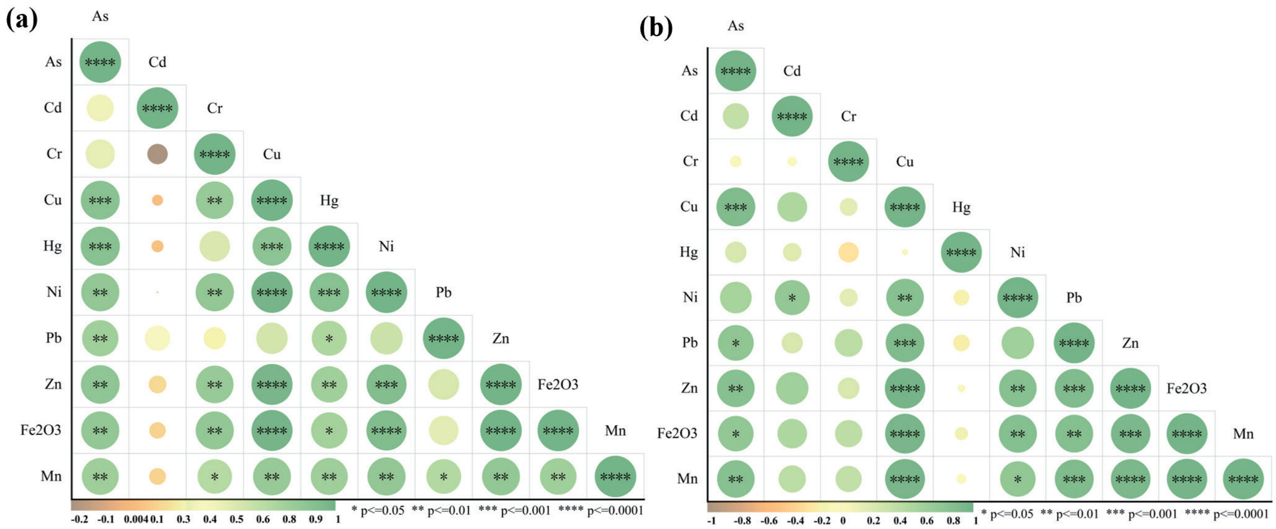

Fig. 5. Pearson correlation analysis of elements in soil profiles. a) based on P1 and P2 data; b) based on P3 and P4 data.

Table 2. Principal component analysis on soil elements.

	P1-P2			P3-P4		
	PC1	PC2	PC3	PC1	PC2	PC3
As	0.340	0.277	-	0.329	0.280	0.358
Cd	-	0.721	0.543	0.231	0.367	-
Cr	0.288	-	-	0.125	-	-
Cu	0.363	-	-	0.385	-	-
Hg	0.331	-	-	-	0.604	0.452
Ni	0.361	-	-	0.338	-	-
Pb	0.258	0.399	-	0.349	-	0.273
Zn	0.356	-	0.287	0.386	-	-
Fe_2O_3	0.352	-	-	0.380	-	-
Mn	0.331	-	-	0.379	-	-
Variance contribution rate (%)	72.997	14.824	6.315	65.153	15.565	9.109
Cumulative variance contribution (%)	72.997	87.821	94.136	65.153	80.718	89.827

in the P1-P2 group, suggesting that the relative importance of other sources increased. PC1 was also associated with As (0.329), Cd (0.231), and Cr (0.125). This indicates that in the P3-P4 area, the distribution of As, Cd, and Cr might be influenced by both natural background and anthropogenic inputs, showing a "mixed" source characteristic. In the P3-P4 group, Hg (0.604) was particularly prominent. It showed no significant correlation with other heavy metals, Fe_2O_3, or Mn (Fig. 5b)), and became the dominant element in PC2 (variance contribution rate 15.565%) in PCA. This independent behavior of Hg indicates the presence of one or more unique and independent anthropogenic sources. This might include historical atmospheric deposition, the use of mercury-containing fungicides, or localized, non-uniform industrial pollution [59]. Its anomalous high value at 100 cm depth in P4 ("Vertical Distribution Characteristics of Heavy Metals in Soil Profiles" and "Pollution Assessment of Heavy Metals in Soil Profiles" Sections) corroborates this analysis, suggesting that its input might have historical legacy characteristics or be related to specific deep geochemical processes. Meanwhile, PC2 was also associated with Cd (0.367) and As (0.280). In the P1-P2 group, Cd and As were the primary anthropogenic signals superimposed on the natural background, with agricultural sources being more likely. However, in the P3-P4 area, besides possible similar agricultural inputs, an independent pollution represented by Hg with more specific sources constitutes another significant anthropogenic pressure, leading to a more complex element source structure. PC3 (variance contribution rate 9.109%) was dominated by Hg (0.452) and As (0.358), reaffirming the complexity of As sources (possibly related to multiple anthropogenic activities), while Pb in the P3-P4 group showed some association with both PC1 and PC3, indicating its sources are also complex. The authors' investigation found that the distribution of Pb might be jointly influenced by historical leaded gasoline residues, regional atmospheric deposition, and agricultural activities [59]. Comprehensive analysis suggests that the authors attribute PC1 to a natural-agricultural mixed source, PC2 to an agricultural-industrial mixed source, and PC3 to an agricultural-industrial-traffic mixed source. Among all anthropogenic sources, Cd and Hg are priority risk elements requiring attention. Cd is due to its high toxicity and widespread introduction through agricultural activities, while Hg poses a potential threat to the environment due to its persistence, high toxicity, and independent point source pollution characteristics.

Conclusions

Systematic geochemical analysis of alluvial soil profiles in Gaotai County, located in the middle reaches of the Heihe River, yielded the following primary conclusions:

(1) The vertical distribution patterns of heavy metals in the soils reveal their distinct environmental behaviors and sources. The enrichment of Cd, Hg, and As indicates significant anthropogenic inputs, whereas the relatively uniform distribution of elements such as Cu and Ni reflects the dominant control of natural parent material. Although the comprehensive Potential Ecological Risk Index (RI) suggests an overall low risk level in the region, Cd and Hg constitute the most significant potential ecological risks currently, due to their high toxicity and bioavailability, and should be prioritized as key targets for environmental management.

(2) Based on the CIA and A-CN-K diagram, it was confirmed that the alluvial soils in the study area have undergone moderate-intensity chemical weathering and widespread potassium metasomatism. This geochemical background not only governs the distribution of major and nutrient elements but also profoundly influences the adsorption, fixation, and migration behaviors of heavy metals through the formation of secondary clay minerals and Fe-Mn oxides, providing a crucial geochemical baseline for distinguishing between natural and anthropogenic sources.

(3) Integrated multivariate statistical analysis successfully identified the multiple sources of heavy metals in the study area. Natural parent material (primarily represented by the PC1 factor) is the fundamental source for elements such as Cu, Ni, and Cr. Anthropogenic sources exhibit spatial heterogeneity: agricultural non-point source pollution, particularly Cd input strongly associated with phosphate fertilizer application, is a prevalent and major anthropogenic contributor across the area. In specific regions (P3-P4), an independent special industrial/historical pollution source, represented by Hg, was identified, the impact of which requires further source tracing and attention. The sources of As, Pb, and Zn demonstrate a mixture of natural and anthropogenic factors.

Based on these findings, the following recommendations are proposed for soil environmental protection in the oasis agricultural areas of the middle Heihe River: First, priority should be given to controlling agricultural non-point source pollution, including promoting the use of low-Cd phosphate fertilizers and regulating the application of pesticides and livestock manure. Second, specialized investigation and monitoring should be conducted in areas with anomalous concentrations of Hg and other elements to clarify their specific sources and historical migration pathways. Finally, it is essential to recognize that within the "two mountains flanking one river" topographical context, the material sources from the southern Qilian Mountains and the agricultural activities in the northern oasis collectively shape the "source-sink" pattern of heavy metals. Future environmental management strategies must fully consider the characteristics of this coupled natural-anthropogenic watershed system. This study provides a significant case reference and methodological framework for preventing and controlling soil heavy metal pollution in agricultural oases of similar inland river basins.

Acknowledgments

This work was financially supported by the Yanzhao Shanshui Science and Technology Fund (KY01202506) and the Geological Survey Project of Ecological Protection and Restoration in the Middle Reach of the Black River Region (DD20242705). We also extend our sincere thanks to our colleagues from the Environmental Geological Survey Office, Langfang Integrated Natural Resources Survey Center, China Geological Survey for their invaluable assistance during the field sampling and laboratory analysis.

Authors' Contributions

Writing – original draft, Yuze Bai.; Writing – review and editing, Yi Liu.; Investigation and Methodology, Ning Zhang, Furong Zhai; Investigation and Validation, Kairan Xu.; Project administration, Miao Liu.; Data curation, Jiaxing Sun, Manman Lin.

Conflict of Interest

The authors declare no conflict of interest.

Data Availability Statement

Data will be made available on request.

References

1. KUMAR S., GOPINATH K.A., SHEORAN S., MEENA R.S., SRINIVASARAO C., BEDWAL S., JANGIR C.K., MRUNALINI K., JAT R., PRAHARAJ C.S. Pulse-based cropping systems for soil health restoration, resources conservation, and nutritional and environmental security in rainfed agroecosystems. Frontiers in Microbiology, **13**, **2023**.
2. YU H., ZHANG Y., TAN W.B., ZHANG Z. Microplastics as an Emerging Environmental Pollutant in Agricultural Soils: Effects on Ecosystems and Human Health. Frontiers in Environmental Science, **10**, **2022**.
3. ZHENG X.J., CHEN M., WANG J.F., LI F.G., LIU Y., LIU Y.C. Ecological Risk Assessment of Heavy Metals in the Vicinity of Tungsten Mining Areas, Southern Jiangxi Province. Soil & Sediment Contamination, **29** (6), 665, **2020**.
4. MIAO F., ZHANG Y., LI Y., LIN Q. A synthetic health risk assessment based on geochemical equilibrium simulation and grid spatial interpolation for zinc (II) species. Journal of Environmental Management, **304**, 114207, **2022**.
5. LIU H.J., XIE J., CHENG Z.F., WU X.L. Characteristics, Chemical Speciation and Health Risk Assessment of Heavy Metals in Paddy Soil and Rice around an Abandoned High-Arsenic Coal Mine Area, Southwest China. Minerals, **13** (5), **2023**.
6. MOHAMOUD A.M., HALDER B., SHAKIR H.S., YASEEN Z.M. Soil heavy metal contamination analysis: A representative case study in New Zealand. Journal of Environmental Chemical Engineering, **13** (3), 116808, **2025**.
7. EJAZ U., KHAN S.M., SHAH S.F.A., KHALID N., JEHANGIR S., RIZVI Z.F., SVENNING J.-C. Integrative data-driven analytics for assessing ecological and human health risks of soil heavy metal contamination. Journal of Hazardous Materials Advances, **17**, 100596, **2025**.
8. HE W., HUANG J., LIU S., SHI L., LI E., HU J., ZHANG W., ZHANG C., PANG H., LIU Z. Co-occurrence of microplastics and heavy metals to urban river sediments: The vertical distribution characterization and comprehensive ecological risk assessment. Journal of Hazardous Materials, **488**, 137500, **2025**.
9. DEMIRELA G., TERZI M.H., DURGUN M.B. Comprehensive assessment of heavy metal contamination in forested and agricultural soils: Distribution patterns, source apportionment, environmental and human health risks. Science of The Total Environment, **1002**, 180647, **2025**.
10. BAO J., CHANG Y., CHENG N., LI Y., CHANG X., FENG J., NAN X., REN H. Vertical distribution and migration of heavy metals in soil of green stormwater infrastructure receiving roof runoff. Science of The Total Environment, **954**, 176511, **2024**.
11. LI T., LI Y.G., LIU H., LI S.M., OUYANG Y., LI C., ZHANG K., LI J., ZHANG J.H., ZHANG T.J., HUANG Y., WU J.Y. Chemical weathering intensity and geochemical characteristics of Cretaceous terrigenous clastic rock-purple soil profiles in the Pushi area, Xichang. Geological Journal, **57** (9), 3587, **2022**.
12. ABUZAID A.S., JAHIN H.S. Profile Distribution and Source Identification of Potentially Toxic Elements in North Nile Delta, Egypt. Soil & Sediment Contamination, **28** (6), 582, **2019**.
13. TAN S., ZHANG T., YANG Z. Vertical distribution patterns and ecological risk assessment of heavy metal(loid)s pollution in a sediment profile from Bohai Sea. Marine Pollution Bulletin, **209**, 117089, **2024**.
14. YANG Z., ZOU Z., TAN S., YAN H. Assessment of historical heavy metal(loid)s contamination records reveals dominant control of grain size effect on the sedimentary profiles from the North Yellow Sea. Environmental Pollution. **385**, 127078, **2025**.
15. CAI G., LI S., ZHAO L. Heavy metal enrichment characteristics in different sedimentary environments: A case study of the Pearl River Estuary and adjacent coastal area. Regional Studies in Marine Science, **85**, 104180, **2025**.
16. BUDIANTA W., AHMAD J.S.M., PRASTISTHO W., HENDRAYANA H., HIDEKI O., HINODE H. Assessment of heavy metal contamination in river stream sediment in urban area: a case study of Yogyakarta City, Indonesia. Environmental Monitoring and Assessment, **197** (7), **2025**.
17. BAL AKKOCA D., YILDIRIM I., AL-JUBOURY A.I. Parent material, weathering and heavy metal contamination in the surface soils from basin infill sediments in Elazığ Industrial Area, Eastern Turkey. Journal of African Earth Sciences, **212**, 105185, **2024**.

18. YAN C., WU Q., LI R., LIANG Z., YANG Z., ZHU A., GAO L. Enrichment features, ecological risks assessment and quantitative sources appointment of sediment heavy metals: An example of the urbanized Xizhi River catchment, South China. Environmental Chemistry and Ecotoxicology, **7**, 263, **2025**.
19. BOUZID K., BATAILLARD P., BEKIRI F., BOULTIF M., BOUTALEB A., CHAIB W., HENNI B. Assessment of soil heavy metal pollution: a case study of the abandoned mine of Ichmoul, Algeria. Environmental Monitoring and Assessment, **197** (4), **2025**.
20. LI J., DUAN H.J., LI J.H., LIU Y., HUANG W.J. Characteristics and health risks of heavy metal pollution in the soil of parks in Kaifeng City. Environmental Geochemistry and Health, **47** (10), **2025**.
21. PAN Y., CHEN M., WANG X., CHEN Y. Ecological risk, source apportionment, and influencing factors of heavy metals in soil in a typical lead-zinc mining watershed, Guangxi, China. Journal of Environmental Chemical Engineering, **12** (3), 112731, **2024**.
22. FU C., LI X., MA J., GAO M., BAI Z., LIU C. Heavy metal(loid)s contamination assessment of soils in Shendong coal base of the Kuye River basin, China: spatial distribution, source identification and ecological risk. Environmental Earth Sciences, **82** (21), 498, **2023**.
23. LI X., ZHANG J., ZHU Y., CHAN S., LIU Y., WU C., ZHUANG D., TAO W., CHEN S. Characteristics and Source Analysis of Heavy Metals in the Surrounding Topsoil of Tuo Lake Nature Reserve. ACS Omega, **10** (29), 31921, **2025**.
24. HAKANSON L. An ecological risk index for aquatic pollution control.a sedimentological approach. Water Research, **14** (8), 975, **1980**.
25. WAN X.Q., WANG C.Y., MA Q.L., YANG C.K., ZHANG J.Z., SHANG Y.T. Analysis of heavy metal contamination in topsoils across land use types within the Manghe River watershed in South Taihang and its source attribution. PLOs One. **20** (10), **2025**.
26. XU L., ZHAO F., XING X., PENG J., WANG J., JI M., LI B.L. A Review on Remediation Technology and the Remediation Evaluation of Heavy Metal-Contaminated Soils. Toxisc, **12** (12), 897, **2024**.
27. ABU M., KALIMENZE J., MVILE B.N., KAZAPOE R.W. Sources and pollution assessment of trace elements in soils of the central, Dodoma region, East Africa: Implication for public health monitoring. Environmental Technology & Innovation, **23**, 101705, **2021**.
28. ZHANG L.L., ZHANG Z.M., MU G.T., HU W., HE L.F. PCA-PMF combined approach for source identification and risk quantification of heavy metals in legacy mining agricultural soils. Environmental Monitoring and Assessment, **197** (11), **2025**.
29. MA L., WANG Y.Q., MA X.W., MA Y., MA Z.Q., PAN Z., BAI Y.R. Analysis of Heavy Metal Contamination, Distribution and Sources in Agricultural Soil of Yellow River Irrigation Area. Geological Journal. **2025**.
30. ZHANG J.Q., NING J.L., HE Z.K., WANG J., LIU Z.J., YAN H.H., LIANG Z.R. Quantitative source apportionment and pollution characteristics of heavy metals in agricultural soils surrounding a legacy Pb-Zn mine. Environmental Earth Sciences, **83** (21), **2024**.
31. BALA N., PAKADE Y.B., MAHURKAR M., KADAVERUGU R., MINAKSHI, KATNORIA J.K. Spatial distribution and source identification of metal contaminants in soil and rice grain samples: a study on exploration of soil quality and risk assessment. Environmental Monitoring and Assessment, **196** (3), **2024**.
32. ZHANG T., WANG P., WANG M., LIU J., GONG L., XIA S. Spatial distribution, source identification, and risk assessment of heavy metals in riparian soils of the Tibetan plateau. Environmental Research, **237**, 116977, **2023**.
33. BASHIR Z., RAJ D., SELVASEMBIAN R. Source profiling, pollution and health risk assessment of heavy metals in agricultural soils around an industrial cluster using PCA and GIS-assisted PMF. Environmental Monitoring and Assessment, **197** (7), 711, **2025**.
34. BUDI H.S., CATALAN OPULENCIA M.J., AFRA A., ABDELBASSET W.K., ABDULLAEV D., MAJDI A., TAHERIAN M., EKRAMI H.A., MOHAMMADI M.J. Source, toxicity and carcinogenic health risk assessment of heavy metals. Reviews on Environmental Health, **39** (1), 77, **2024**.
35. NIE X.-Y., WANG C., LI K.-M., GAO F.-Y., HUANG W.-Z., LI X. Spatiotemporal analysis of landscape ecological risk and its influencing factors based on land cover changes in the Hexi Corridor, Northwest China, 2000–2020. Environmental and Sustainability Indicators, **28**, 100888, **2025**.
36. YAN Y., GUAN Q., SHAO W., WANG Q., YANG X., LUO H. Spatiotemporal dynamics and driving mechanism of arable ecosystem stability in arid and semi-arid areas based on Pressure-Buffer-Response process. Journal of Cleaner Production, **421**, 138553, **2023**.
37. TING L., JIA X.P., YAN Z., LIAO X.H., PAN K.J., ZHANG Z.C. Characteristics, sources, diffusion, and risk assessment of heavy metals pollution in topsoil of typical gobi in the Hexi Corridor, Northwestern China. Journal of Soils and Sediments, **25** (4), 1074, **2025**.
38. LUO H., YANG L., ZHANG C., XIAO X., LYU X. Early warning of heavy metals contamination in agricultural soils: Spatio-temporal distribution and future trends in the Hexi Corridor. Ecological Indicators, **160**, 111908, **2024**.
39. WANG F., GUAN Q., TIAN J., LIN J., YANG Y., YANG L., PAN N. Contamination characteristics, source apportionment, and health risk assessment of heavy metals in agricultural soil in the Hexi Corridor. CATENA, **191**, 104573, **2020**.
40. HUANG J.L., TIAN Y.Q., LIU Z.F., LI Z.X., SUN S.Y., SU Z.W., DAI H.M. Contamination and source-specific health risk assessment of soil heavy metals in the middle and upper reaches of the Heihe River Basin of China. Environmental Geochemistry and Health, **47** (4), **2025**.
41. WANG Y., LI B.L., LI J.P., WANG Z.H., XIAN F.Y., FAN Y.Y. Spatial distribution characteristics and pollution levels of heavy metals in surface water and sediments of the Heihe cascade reservoir system, China. Water Supply, **22** (11), 8353, **2022**.
42. WEI L., TIAN S., LU Q., ZHONG Y., ZHENG Y., LU Y., XIAO Z. Estimating soil organic carbon content of multiple soil horizons in the middle and upper reaches of the Heihe River Basin. CATENA, **234**, 107574, **2024**.
43. DASH S., BORAH S.S., KALAMDHAD A.S. Heavy metal pollution and potential ecological risk assessment for surficial sediments of Deepor Beel, India. Ecological Indicators, **122**, 107265, **2021**.
44. NESBITT H.W., YOUNG G.M. Early Proterozoic climates and plate motions inferred from major element chemistry of lutites. Nature, **299** (5885), 715, **1982**.
45. WANG C., SHI M.Q., WANG J.H., ZHONG C. Geochemical characteristics of metal(loid)s in forest soil

profiles affected by Pb-Zn ore mining. Journal of Cleaner Production, **501**, **2025**.
46. MCLENNAN S.M. Weathering and Global Denudation. The Journal of Geology, **101** (2), 295, **1993**.
47. CHEN M., LI X., CAO X., YANG W., WU P., HAO H., FEI Z., GAO Y. Soil-forming accumulation of heavy metals in geological high background areas: Constraints of structure, lithology, and overlying soil geochemistry. Journal of Geochemical Exploration, **263**, 107518, **2024**.
48. ZHANG Y., SONG B., ZHOU Z. Pollution assessment and source apportionment of heavy metals in soil from lead – Zinc mining areas of south China. Journal of Environmental Chemical Engineering, **11** (2), 109320, **2023**.
49. WAN Y., LIU J., ZHUANG Z., WANG Q., LI H. Heavy Metals in Agricultural Soils: Sources, Influencing Factors, and Remediation Strategies. Toxics, 12 (1), 63, **2024**.
50. WEI M., PAN A., MA R., WANG H. Distribution characteristics, source analysis and health risk assessment of heavy metals in farmland soil in Shiquan County, Shaanxi Province. Process Safety and Environmental Protection, **171**, 225, **2023**.
51. CHI H., LIU X., YANG X., ZHANG R., XIA T., SUN Y., HU K., HAO F., LIU Y., YANG S., DENG Q., WEN X. Risk assessment and source identification of soil heavy metals: a case study of farmland soil along a river in the southeast of a mining area in Southwest China. Environmental Geochemistry and Health, **46** (2), 39, **2024**.
52. YUAN S., YANG G., ZHANG X., LUO S., YAN J., YU Z., DONG H., ZHOU Y. Assessment of distribution, contamination, ecological risks, and sources of heavy metals in soil from metal recycling sites. Environmental Monitoring and Assessment, **197** (6), 630, **2025**.
53. TAYLOR S.G., BRADLEY C.E. Optimal Ordering Strategies for Announced Price Increases. Operations Research, **33** (2), 312, **1985**.
54. XIE N., KANG C., FENG B.Z., ZHANG B. Insight of heavy metal contamination of soil in high background area: field investigation and laboratory test. International Journal of Environmental Science and Technology, **22** (5), 2833, **2025**.
55. ALGEO T.J., HONG H.L., WANG C.W. The chemical index of alteration (CIA) and interpretation of ACNK diagrams. Chemical Geology, **671**, **2025**.
56. HU H.R., LI X., GAO X.Y., WANG L., LI B., ZHAN F.D., HE Y.M., QIN L., LIANG X.R. A review on the multifaceted effects of δ-MnO_2 on heavy metals, organic matter, and other soil components. Rsc Advances, **14** (51), 37752, **2024**.
57. KUN Z., CAI Y.K., CHEN W.D., PENG P.H. Source identification and spatial distribution of heavy metals in soil of central urban area of Chongqing, China. Soil & Sediment Contamination, **32** (6), 771, **2023**.
58. DU H., WANG J., WANG Y., YAO Y., LIU X., ZHOU Y. Contamination characteristics, source analysis, and spatial prediction of soil heavy metal concentrations on the Qinghai-Tibet Plateau. Journal of Soils and Sediments, **23** (5), 2202, **2023**.
59. ZHANG X., ZHANG S., WEI X., LIU Z., WANG C., MU H., HAN Y., LIU C. Identification of sources and analysis of spatial distribution of soil heavy metals in northern China coal mining areas. Environmental Geochemistry and Health, **46** (3), 94, **2024**.